ResearchGate

See discussions, stats, and author profiles for this publication at: https://www.researchgate.net/publication/276467257

Simulation of the Swelling of High-Volatile Bituminous Coal during Pyrolysis. Part 2: Influence of the Maximum Particle Temperature

ARTICLE *in* ENERGY & FUELS · MAY 2015

Impact Factor: 2.79 · DOI: 10.1021/acs.energyfuels.5b00609

CITATION
1

READS
17

4 AUTHORS, INCLUDING:

He Yang
Dalian University of Technology
5 PUBLICATIONS **14** CITATIONS
SEE PROFILE

Sufen Li
Dalian University of Technology
18 PUBLICATIONS **52** CITATIONS
SEE PROFILE

Thomas H. Fletcher
Brigham Young University - Provo Main Campus
155 PUBLICATIONS **2,299** CITATIONS
SEE PROFILE

Available from: He Yang
Retrieved on: 02 February 2016

energy&fuels

Article

pubs.acs.org/EF

Simulation of the Swelling of High-Volatile Bituminous Coal during Pyrolysis. Part 2: Influence of the Maximum Particle Temperature

He Yang,[†] Sufen Li,*[,†] Thomas H. Fletcher,[‡] and Ming Dong[†]

[†]School of Energy and Power Engineering, Dalian University of Technology, Dalian, Liaoning 116024, People's Republic of China

[‡]Chemical Engineering Department, Brigham Young University, Provo, Utah 84602, United States

ABSTRACT: A model was established previously to predict the swelling ratio of high-volatile bituminous coal during pyrolysis based on the assumption that the structure of bubble distribution in the particle at the beginning of the plastic stage is a central bubble surrounded by many surrounding bubbles. The initial number and size of the bubbles when the particles become plastic are calculated by the pressure in the particle, and the chemical percolation devolatilization (CPD) model is used to describe pyrolysis. In this paper, to obtain accurate results at low pyrolysis temperatures, the previous model is improved and the following parts in the model are adjusted: (1) the method for estimating the volume of macropores in the particle at the beginning of swelling and (2) a correlation between the initial bubble number and the particle diameter. The swelling behavior of eight bituminous coals from the literature spanning a wide range of gas temperatures and gas pressures was simulated to test the suitability of the model. The influence of the maximum particle temperature during pyrolysis (T_{max}) on swelling is analyzed. The predicted particle swelling for a Pittsburgh #8 bituminous coal particle during pyrolysis increases with T_{max} up to about 950 K, decreases as T_{max} increases from 950 to 1100 K, and then changes little with further increases in T_{max}. The influence of T_{max} coupled with the heating rate makes the swelling ratio in experiments from the literature increase from 1.07 to 1.51 as T_{max} increases from 840 to 952 K and the heating rate increases from 1.38×10^4 to 2.18×10^4 K/s. Particle swelling decreases from 1.51 to 0.95 as T_{max} decreases from 952 to 1662 K and the heating rate increases from 2.18×10^4 to 2.24×10^5 K/s. At a constant heating rate of 1×10^4 K/s, when T_{max} is larger than 950 K, the predicted particle swelling during pyrolysis increases and then decreases with increasing ambient pressure. However, when T_{max} is smaller than 950 K, the predicted particle swelling during pyrolysis decreases with increasing ambient pressure.

1. INTRODUCTION

Swelling during coal pyrolysis influences the porosity, inner surface area, and density of the particle.[1−3] The studies on swelling have focused on the influence of the particle heating rate and ambient pressure. Studies at low heating rates in thermogravimetric analyzers (TGAs) and wire mesh reactors indicate that the final swelling ratio of the coal particle increases with increasing heating rate.[4] However, studies with drop-tube furnaces and flat-flame burners show that the swelling ratios decrease at rapid heating rates.[5,6] Studies in elevated pressure reactors indicate that the coal swelling ratio also has the same increasing and then decreasing trend with increasing ambient pressure.[2,7,8] However, less work has examined the influence of T_{max} during pyrolysis.

The maximum particle temperature is determined by the temperature of gases surrounding the particle. It was usually considered that ambient temperature influences swelling through the effect on the heating rate.[9,10] However, T_{max} is an important reaction condition, and it determines the completeness of aliphatic structure cracking and the volatile yield during pyrolysis. It is difficult to study the effect of the heating rate or ambient pressure on swelling independently of the particle temperature in entrained flow experiments, because the heating rate is changed by changing the gas temperature, and hence, T_{max} and the heating rate are coupled.

A few models have been developed by different investigators to describe the swelling of coal particles, such as the single-bubble model[11,12] and the multi-bubble model.[13−15] The single model cannot explain the phenomenon that the number of bubbles in the particle changes with the heating condition[16] and cannot predict the decreasing trend of the particle size during the late stage of pyrolysis at rapid heating rates. The multi-bubble model cannot predict the decrease in swelling with increasing heating rate at the heating rate greater than 10^4 K/s. In a previous paper,[17] a model was established to predict the swelling ratio of high-volatile bituminous coal during pyrolysis based on the assumption that the structure of bubble distribution in the particle at the beginning of the plastic stage is a central bubble surrounded by many surrounding bubbles. The initial number and size of the bubbles when the particles become plastic were calculated by the pressure in the particle.[18] The model predicts experimentally observed trends in the swelling ratio with the heating rate; particle swelling during pyrolysis increases with the heating rate up to about 10^4 K/s and then decreases with further increases in the heating rate. Predictions of increasing and then decreasing swelling with increases in the ambient pressure also agree with trends observed experimentally. However, the influence of T_{max} was not analyzed in previous research. The change of the swelling ratio with the heating rate predicted at a constant T_{max} is smaller than under the experimental temperature history

Received: March 23, 2015
Revised: May 12, 2015
Published: May 12, 2015

ACS Publications © 2015 American Chemical Society

DOI: 10.1021/acs.energyfuels.5b00609
Energy Fuels 2015, 29, 3953−3962

(where T_{max} changes at each heating rate[2,5,8,9,19,20]), implying that T_{max} influences swelling independent of the heating rate.

This paper describes improvements to a previous model,[17] to provide more accurate results at low pyrolysis temperatures. Improvements were made to the calculation model for the particle porosity before swelling, the method for estimating the volume of macropores in the particle at the beginning of swelling, and the correlation between the initial bubble number and the particle diameter. In addition, the influence of T_{max} on swelling is analyzed.

2. MODELING

2.1. Review of the Previous Swelling Model. *2.1.1. Chemical Percolation Devolatilization (CPD).* In this paper, the pyrolysis reaction is described by the CPD model.[21−23] The CPD model includes (a) a description of the chemical structure of the parent coal, (b) a kinetic scheme for breaking labile bonds and side chains, (c) percolation statistics based on a Bethe lattice for freeing molecules from the coal particle, (d) a vapor−liquid equilibrium treatment of metaplast versus tar, and (e) a cross-linking mechanism for reattaching metaplast to the solid char.

2.1.2. Viscosity of the Coal Particle. During pyrolysis, the viscosity of the thermoplastic coal particle first increases and then decreases,[24,25] and when the viscosity of the coal particle is smaller than a specified value, the particle becomes plastic.[12,13] Devolatilization is divided into three stages: the preplastic stage, the plastic stage, and the resolidified stage. The temperature-dependent viscosity of the coal particle is expressed as shown in eq 1,[12,13,15] where ϕ_m is the metaplast content in the coal metaplast and T is set to 723 K when $T > 723$ K. The critical viscosity value in this work is set to 1×10^4 Pa s.

$$\mu_{coal} = \frac{1 \times 10^{-11} \exp(45000/RT)}{((1 - \varphi_m)^{-1/3} - 1.0)} \tag{1}$$

2.1.3. Initial Number of Bubbles. The macropores surrounded by continuous metaplast can convert to bubbles, and the initial number of bubbles at pressure P_i can be described by eq 2, where f^i_{volume} is the volume fraction at pressure P_i, m^{pc}_p is the initial mass of the coal particle, and $\hat{V}_{pore}$ is the volume of macropores per unit mass of coal at the beginning of the plastic stage.

$$n^i_{b0} = \frac{\hat{V}^0_{pore} m^{pc}_p f^i_{volume}}{4/3\pi r^{i\ 3}_{b0}} \varphi_m f_{VP} \tag{2}$$

The initial radius of the bubble under the pressure P_i is described as eq 3, where f_r is the adjustable parameter, $0 \le f_r \le 1$, and is set to 0.5 in this paper.

$$r^i_{b0} = f_r \frac{2\sigma}{P_i - P_\infty} + (1 - f_r) r_{pore} \tag{3}$$

2.1.4. Growth Rate of Bubbles. The growth rate of bubbles is described by a force balance,[12,13,15] as shown in eq 4, where r_b is the radius of the bubble, P_∞ is the ambient pressure, P_b is the pressure in the bubble, and σ is the surface tension of coal metaplast.

$$\frac{dr_b}{dt} = \frac{r_b}{4\mu_{coal}} \left(P_b - P_\infty - \frac{2\sigma}{r_b} \right) \tag{4}$$

2.1.5. Change in Bubble Number. Changes in the number of bubbles can happen by bubble rupture or bubble coalescence. Treatments of these effects are described below.

The rupture rate of the surrounding bubbles on the particle surface is as shown in eq 5, where R_p and R_{p0} are the radii of the particle and its initial value.

$$\left(\frac{dn_b}{dt} \right)_r = -\frac{4\pi (R_p - r_b)^2}{\frac{4\pi}{3} R^3_{p0}} \frac{dr_b}{dt} n_b \tag{5}$$

The coalescence rate of surrounding bubbles with the center bubble is estimated as shown in eq 6, where r_c is the radius of the center bubble.

$$\left(\frac{dn_b}{dt} \right)_c = -\frac{4\pi (r_c + r_b)^2}{\frac{4\pi}{3} R^3_{p0}} \frac{d(r_b + r_c)}{dt} n_b \tag{6}$$

2.1.6. Rupture of the Central Bubble. During the single-bubble stage, as the internal pressure increases to a specified value, the bubble ruptures. The criteria for bubble rupture are defined using wall strength,[12] as shown in eq 7. The critical wall stress, S_w, is set to $(P_\infty / 1.02325 \times 10^5)^{2/3} \times 1.02325 \times 10^5$ Pa.

$$\frac{1.5 r^3_b (P_b - P_\infty)}{R^3_p - r^3_b} - P_\infty > S_w \tag{7}$$

2.2. Modification of the Model. To improve swelling predictions of the previous model at lower temperatures, the following changes were made: (1) the method for estimating the volume of macropores in the particle at the beginning of swelling and (2) the correlation between the initial bubble number and the particle diameter. In addition, the method for calculating the porosity of high-volatile bituminous coal during pyrolysis is proposed.

2.2.1. Volume of Macropores at the Beginning of Swelling. The volume of macropores at the beginning of swelling is calculated as follows:

$$\hat{V}^0_{pore} = \hat{V}^{pc}_{pore} \frac{\theta}{\theta_{pc}} \tag{8}$$

where θ and θ_{pc} are the porosities of the coal particle and its initial value, respectively.

$\hat{V}^{pc}_{pore}$ was set to 2.4×10^{-5} m^3/kg in previous work, which is the average volume of macropores in parent bituminous coals.[26] However, the value of $\hat{V}^{pc}_{pore}$ varies for different bituminous coals. In this work, the porosity (θ_{pc}) of the particular bituminous coal is used to improve the accuracy of the calculation as follows:

$$\hat{V}^{pc}_{pore} = 2.4 \times 10^{-5} \frac{\theta_{pc}}{\theta^m_{pc}} \tag{9}$$

where θ^m_{pc} is the average porosity of various raw bituminous coals.

2.2.2. Correlation between the Initial Bubble Number and the Particle Diameter. During pyrolysis, the solid phase and the metaplast are distributed throughout the particle. If the distance between two groups of metaplast is large enough to make them unable to connect with each other, they cannot trap the pore volume to form a bubble. In a larger particle, the metaplast groups may be more dispersed, and therefore, there should be a factor related to the volume of the particle that changes the bubble formation. An influence factor for particle volume, f_{VP}, is therefore used to correct the number of bubbles as follows:

$$f_{VP} = \left(\frac{15 \times 10^{-6}}{R_{p0}} \right)^3 \tag{10}$$

The form of eq 10 was obtained from fitting experimental data.

2.2.3. Porosity. 2.2.3.1. Preplastic Stage. During the preplastic stage, with increasing spaces left by volatiles in the particle and the opening of closed pores, the pores are expanded. The porosity is then calculated as follows:

$$\theta = \theta_{pc} + (1 - \theta_{pc})[(f_{tar} + f_{gas})(1 - f_{CP})(1 - A_{dry}) + f_{CP}(1 - p/p_0)] \tag{11}$$

where f_{CP} is the initial volume fraction of closed pores in the parent coal, A_{dry} is ash content on a dry basis, p and p_0 are the fractions of intact bridges and its initial value, respectively, and f_{gas} and f_{tar} are the yields of gas and tar on a dry and ash-free basis, respectively.

DOI: 10.1021/acs.energyfuels.5b00609
Energy Fuels 2015, 29, 3953−3962

Table 1. Coal Parameters

coal	C_{daf} (%)	H_{daf} (%)	N_{daf} (%)	O_{daf} (%)	V_{daf} (%)	A_{ad} (%)
Illinois #6	76.68	5.54	1.45	12.73	44.27	8.46
Pittsburgh #8	84.2	5.50	1.70	7.60	37.10	3.74
Blue #1	75.6	5.26	1.32	0.49	17.33	3.48
Hiawatha Bituminous	79.69	5.27	1.22	13.38	37.24	7.17
Eastern Bituminous	79.08	5.84	1.49	12.59	47.87	7.36
Australian Bituminous	83.7	5.45	1.81	8.6	30.4	15.1
Adaville #1	70.64	5.32	1.03	21.98	44.57	3.33
Kentucky #9	77.01	5.61	1.69	11.69	46.27	8.07

Table 2. Chemical Structure Parameters of the Parent Coal

coal	p_0	c_0	M_{clust} (g/mol)	M_δ (g/mol)	$\sigma + 1$
Illinois #6	0.47	0.00	408.38	33.68	5.12
Pittsburgh #8	0.52	0.00	349.71	22.88	4.88
Blue #1	0.54	0.07	350.24	36.16	5.00
Hiawatha Bituminous	0.56	0.01	341.78	28.46	5.00
Eastern Bituminous	0.46	0.02	402.57	32.05	4.94
Australian Bituminous	0.56	0.00	347.92	22.76	4.82
Adaville #1	0.57	0.13	380.88	47.25	4.63
Kentucky #9	0.44	0.00	415.68	33.19	5.18

2.2.3.2. Plastic Stage. During the plastic stage, the bubbles occupy the main part of the coal particle and the particle radius is shown in eq 12

$$R_p = \left\{ \sum n_b r_b^3 + \frac{(1 - f_{tar} - f_{gas}) m_{P0} (1 - A_{dry})}{4\pi \rho_{melted}/3} \right\}^{1/3} \quad (12)$$

where ρ_{melted} is the density of the melted coal (not including the volume of bubbles).

The pores in the particle consist of the bubbles and the pores not transformed into bubbles at the beginning of swelling, and the porosity is as follows:

$$\theta = \left(\sum n_b r_b^3 + R_{p0}^3 \theta_{melt}^0 - \sum n_b^0 r_b^{0^3} \right) / R_p^3 \quad (13)$$

where θ_{melt}^0 is the coal particle porosity at the beginning of swelling and n_b^0 and r_b^0 are the initial bubble number and radius at the beginning of swelling, respectively.

2.2.3.3. Resolidified Stage. During the resolidified stage, the increasing spaces left by volatiles in the particle and the opening of the closed pores increase the volume of pores in the particle. The porosity is as follows:

$$\theta = \theta_{melt}^e + (1 - \theta_{pc})[(f_{tar} + f_{gas} - f_{tar-melt}^e - f_{gas-melt}^e) (1 - f_{CP})(1 - A_{ad}) + f_{CP}(p_e - p)/p_{pc}] \quad (14)$$

where θ_{melt}^e, $f_{tar-melt}^e$, $f_{gas-melt}^e$, and p_e are the particle porosity, tar yield, light gas yield, and fraction of intact bridges at the end of the swelling.

2.3. Calculation Conditions. The swelling behavior of eight bituminous coals from the literature were considered spanning a wide range of gas temperatures and gas pressures. The coals were Illinois #6,[4,7,8,19] Pittsburgh #8,[2,5,8,19] Blue #1,[6,19] Hiawatha Bituminous,[6] Eastern Bituminous,[6] Australian Bituminous,[15] Adaville #1,[8] and Kentucky #9.[8] The coal parameters are shown in Table 1. The chemical structure parameters of the parent coal shown in Table 2 are calculated from a correlation[27] developed for use with the CPD model.

The heating rates for these experiments varied from 1×10^3 to 2.24×10^5 K/s; ambient pressure varied from 0.84 to 15 atm; and particle sizes ranged from 58 to 275 μm, as shown in Table 3.

In addition, the changes of swelling with increasing T_{max} of a 69 μm Pittsburgh #8 bituminous coal particle at various heating rates and various heating ambient pressures are calculated to analyze the effects of heating conditions on swelling. It is assumed that, during each heating process, the heating rate was constant. In this case, the particle was heated to T_{max} and then held at that temperature until 480 ms had elapsed.

3. RESULTS AND DISCUSSION

3.1. Validation of the Model. The swelling ratios of the eight high-volatile bituminous coals described in Tables 1−3 were compared to the corresponding experimental data.[2,4−8,15,19] Note that each experiment had different heating conditions, as described above. After the parameter adjustment in this work, most of the results still generally agree with the experimental results, as shown in Figure 1.

3.2. Influence of the Heating Rate. The swelling ratio and porosity of the particle during pyrolysis increase and then decrease with the increasing heating rate.[6,8] At very high heating rates, the bubbles in the particle rupture completely, and because of the rapid internal pressure change, the particle shrinks. In addition, the large weight loss consumes the outside particle boundary, causing a diameter decrease. The model predicts experimentally observed trends of the Pittsburgh #8 bituminous coal particle in the swelling ratio with the heating rate, as shown in Figures 2 and 3. The data points in these two figures are for Pittsburgh #8 bituminous coal at 1 atm. When the temperature histories used in the calculations are the actual temperature histories reported in the experiments (rather than a constant heating rate), the predicted trend agrees with the trend observed in the experiments.

The change of swelling with the heating rate is mainly caused by the changing initial bubble number with increasing heating rate, as shown in Figure 4. At higher heating rates, the reaction is concentrated into a shorter time. The initial average pressure in the particle of the plastic stage increases with increasing heating rate. At higher pressures, the initial diameter of the bubble is small, and hence, the number of bubbles is larger at a certain pore volume. However, the initial size of the central bubble increases with the increasing heating rate, which, in turn, decreases the volume of pores, which can transform to surrounding bubbles, and the initial number of bubbles is therefore decreased.[17]

DOI: 10.1021/acs.energyfuels.5b00609
Energy Fuels 2015, 29, 3953−3962

Table 3. Heating Conditions

coal	diameter (μm)	temperature (K)	heating rate (K/s)	pressure (atm)
Australian Bituminous	70	1573	1.60×10^4	1
	76.5	1573	6.60×10^4	1
	76.5	1573	6.60×10^4	5
	76.5	1573	6.60×10^4	10
	76.5	1573	6.60×10^4	15
	70	1573	1.60×10^4	1
	70	1573	1.60×10^4	20
Illinois #6	115.5	1250	1.69×10^4	1
	275	950	1.00×10^3	1
	62	1189	1.00×10^4	1
	62	1189	1.00×10^4	8
	62	1189	1.00×10^4	22.7
	62	1189	1.00×10^4	37.2
	59.5	1662	1.54×10^4	0.84
	59.5	1798	1.18×10^5	5
	59.5	1907	1.59×10^5	10
	59.5	1834	1.37×10^5	15
Pittsburgh #8	115.5	1050	1.38×10^4	1
	115.5	1250	5.76×10^4	1
	63	986	3.53×10^4	1
	63	1333	5.38×10^4	1
	63	1333	5.38×10^4	1
	75	952	2.18×10^4	1
	75	975	1.98×10^4	1
	69	840	1.73×10^4	1
	63	1106	3.29×10^4	1
	63	1627	6.61×10^4	1
	75	1573	1.00×10^5	1
	75	1573	1.00×10^5	6
	75	1573	1.00×10^5	10
	75	1573	1.00×10^5	15
	60	1662	2.24×10^5	0.84
	60	1798	9.84×10^4	5
	60	1907	1.17×10^5	10
	60	1834	1.01×10^5	15
Blue #1	115.5	1250	5.90×10^4	1
	115.5	1050	1.95×10^4	1
Hiawatha Bituminous	115.5	1250	5.29×10^4	1
Eastern Bituminous	163	1546	2.40×10^4	1
	96.5	1546	6.50×10^4	1
	59.5	1546	1.50×10^5	1
Kentucky #9	60	1662	1.51×10^5	0.84
	60	1798	1.21×10^5	5
	60	1907	1.42×10^5	10
	60	1834	1.24×10^5	15
Adaville #1	58	1662	1.89×10^5	0.84
	58	1907	1.34×10^5	10
	58	1834	1.18×10^5	15

In these entrained flow experiments, the heating rates were changed by changing ambient temperature, and therefore, T_{max} changes for each experiment. The change of the swelling with increasing heating rate is also influenced by T_{max}. The calculated changes of the particle swelling ratio and porosity with increasing heating rate at a constant values of T_{max} are compared to the results computed using the actual experimental conditions. The Pittsburgh #8 bituminous coal

DOI: 10.1021/acs.energyfuels.5b00609
Energy Fuels 2015, 29, 3953−3962

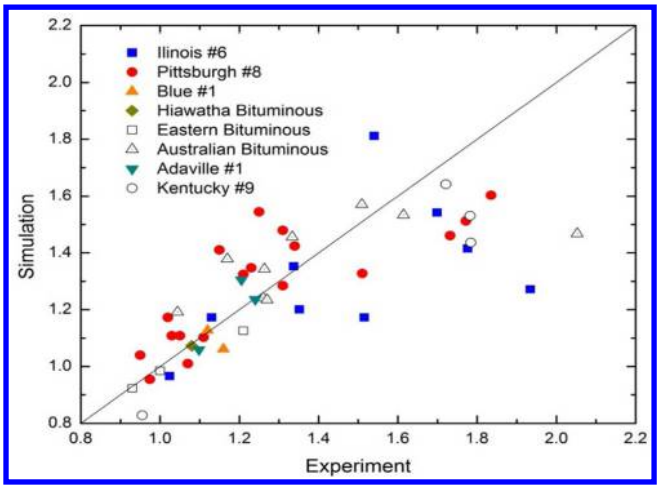

Figure 1. Comparison of the predicted and measured coal particle swelling ratio for the eight coals described in Tables 1−3.[2,4−8,15,19]

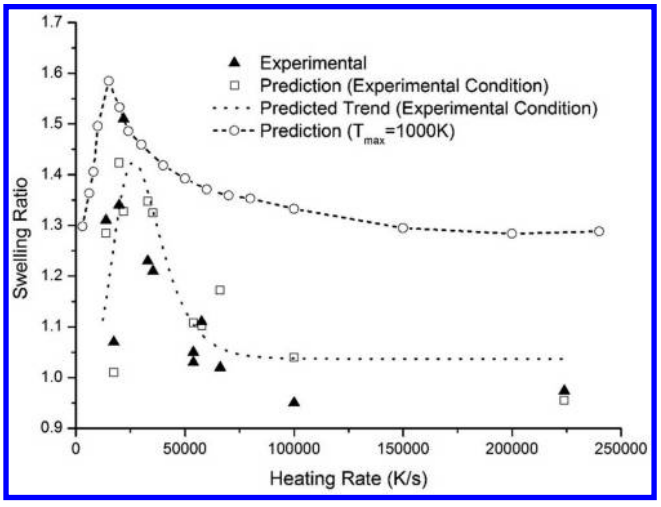

Figure 2. Comparison of the predicted trend of the swelling ratio during pyrolysis with the increase of the heating rate to experimental data.[2,5,8,9,19,20]

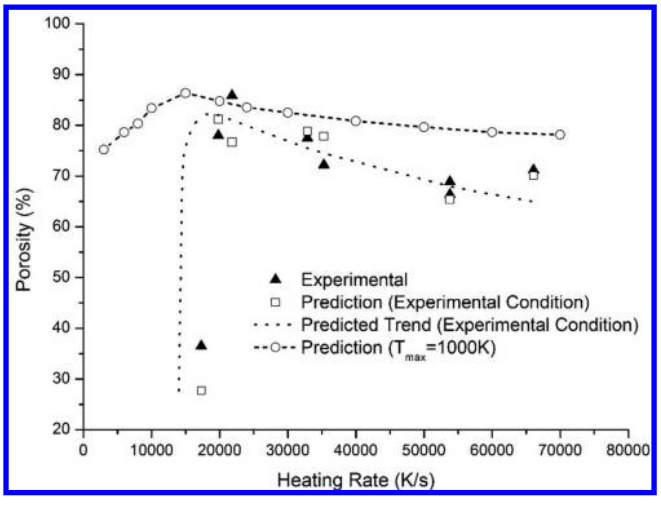

Figure 3. Comparison of the predicted trend of porosity during pyrolysis with the increase of the heating rate to experimental data.[5,20]

particles are heated at various heating rates from 300 to 1000 K and then held at the final temperature until 480 ms elapsed

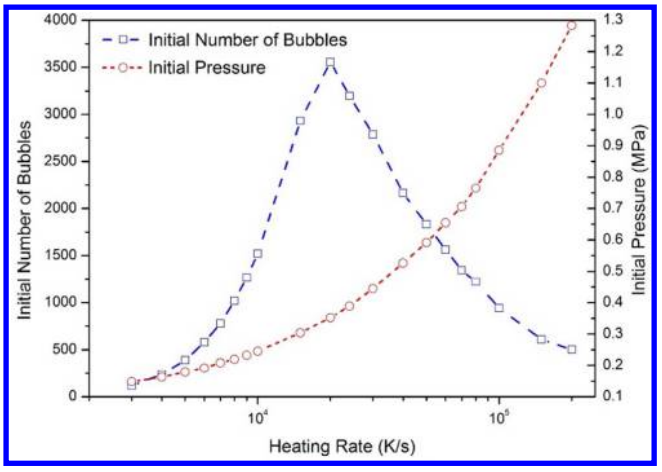

Figure 4. Change of the initial bubble number and initial pressure in the plastic stage with increase of heating rates (T_{max} = 1000 K, and P_{∞} = 0.1 MPa).

time. At the same value of T_{max}, the changes of swelling ratio and porosity with increasing heating rate are smaller than observed in the experimental condition, which indicates that T_{max} influences swelling independent of the heating rate.

3.3. Influence of the Maximum Particle Temperature.

The swelling ratios and porosities of Pittsburgh #8 during pyrolysis at various T_{max} values are compared in Figures 5 and

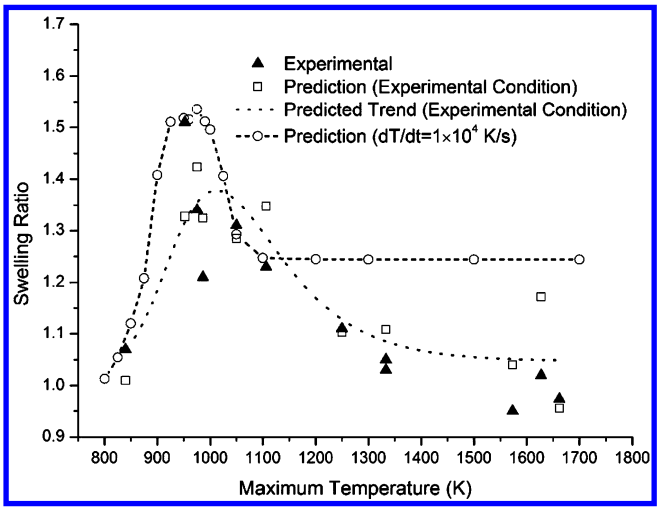

Figure 5. Comparison of the predicted trend of the swelling ratio during pyrolysis with the increase of T_{max} to experimental data.[2,5,8,9,19,20]

6. The swelling ratios and porosities in the experiments increase and then decrease with the increasing T_{max}. The results predicted using the experimental temperature histories compare well to the experimental results. In addition, the changes of the particle swelling ratio and porosity with T_{max} at a constant heating rate are added in the comparison in Figures 5 and 6. The Pittsburgh #8 bituminous coal particles are heated at 1×10^4 K/s from 300 K to various values of T_{max} and then held at that temperature until 480 ms had elapsed. At this constant heating rate, the swelling ratio and porosity increase with T_{max} up to about 950 K and decrease with increasing T_{max} from 950 to 1100 K. However, little change in the swelling ratio occurs with further increases in T_{max}.

DOI: 10.1021/acs.energyfuels.5b00609
Energy Fuels 2015, 29, 3953−3962

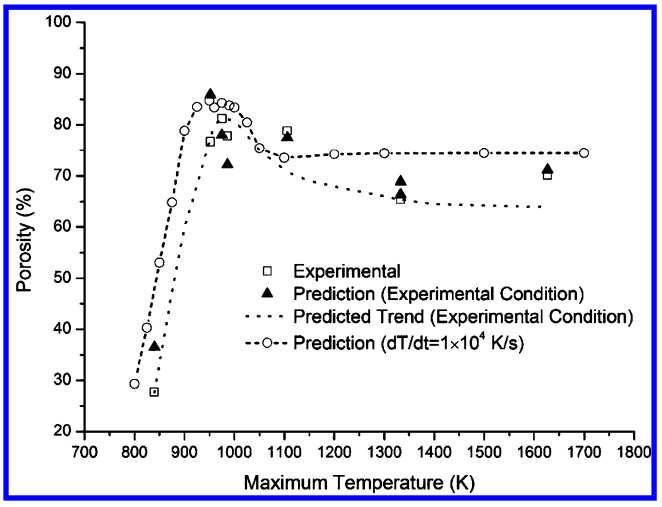

Figure 6. Comparison of the predicted trend of porosity during pyrolysis with the increase of T_{max} to experimental data.[5,20]

T_{max} influences the volatile yield, particle viscosity, and initial bubble number in the particle in the plastic stage during pyrolysis.

3.3.1. Influence of T_{max} on the Volatile Yield. A higher temperature can provide more energy for the cracking of bridges and side chains to generate more light gases, and a higher temperature can also increase the vaporization of metaplast. Therefore, the volatile yield increases with increasing T_{max}, as shown in Figures 7 and 8, until a T_{max} of 1100 K, which is high enough for most of the labile bridges to be cleaved. The volatile yield changes little with a further increase of T_{max}.

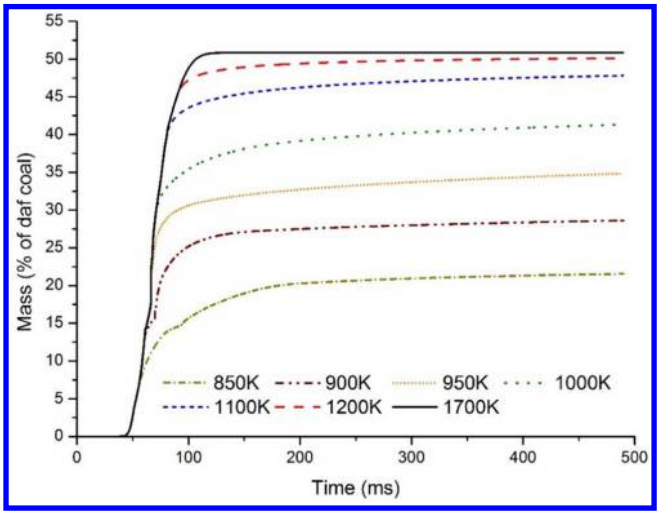

Figure 7. Predicted changes of the volatile yield during pyrolysis at various T_{max} values (heating rate = 1×10^4 K/s, and ambient pressure = 0.1 MPa).

The pressure in the bubble is increased with increasing volatile yield, which, in turn, increases the particle swelling. However, too high of pressure will raise the rupture frequency and, hence, decreases particle swelling.

3.3.2. Influence of T_{max} on Particle Viscosity. The increase of the temperature can provide more energy for the cracking of bridges and side chains to generate more metaplast, which, in turn, decreases the particle viscosity. However, a higher temperature can also increase the vaporization of metaplast

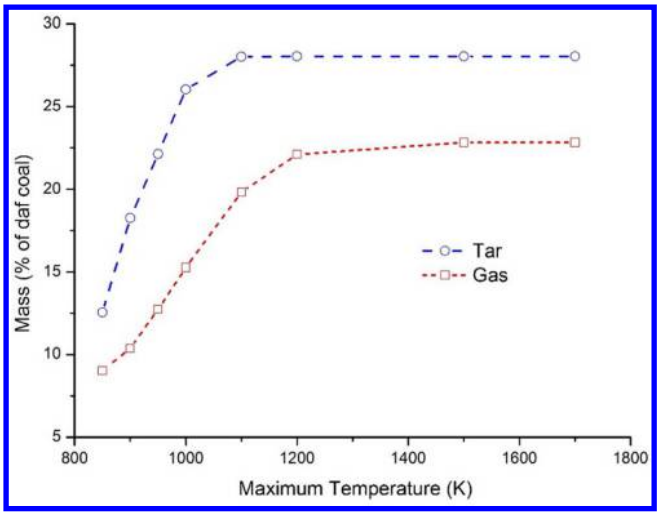

Figure 8. Predicted changes of the final yield of tar and light gas during pyrolysis with increasing T_{max} (heating rate = 1×10^4 K/s, and ambient pressure = 0.1 MPa).

and the cross-linking rate, which, in turn, increases the particle viscosity. The changes of the amount of metaplast in the particle during pyrolysis at a heating rate of 1×10^4 K/s, ambient pressure of 0.1 MPa, and various T_{max} values are shown in Figure 9. At a T_{max} lower than 1100 K, the maximum

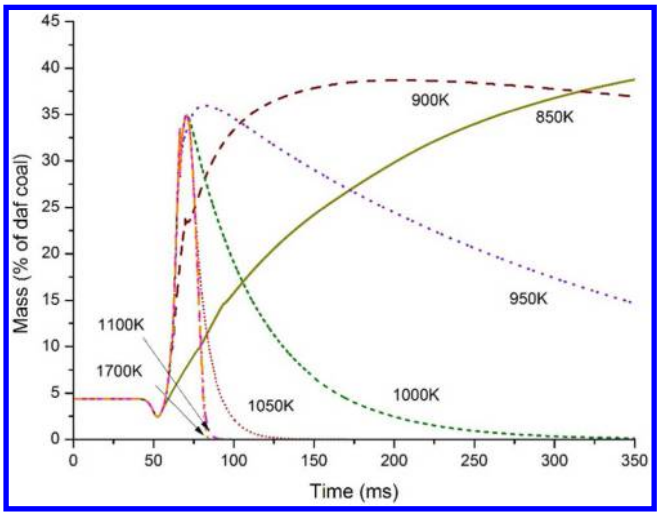

Figure 9. Predicted changes of the metaplast content in the particle during pyrolysis with increasing T_{max} (heating rate = 1×10^4 K/s, and ambient pressure = 0.1 MPa).

metaplast content during pyrolysis decreases with increasing T_{max}. However, the peak metaplast content and particle viscosity appear earlier at higher T_{max}. The amount of metaplast cross-linked to the coal matrix is shown in Figure 10. The changes in the particle viscosity are shown in Figure 11. At T_{max} higher than 1100 K, all of the metaplast is vaporized or cross-linked soon after generation, and before the particle reaches T_{max}, the particle has been resolidified, making the changes of the particle viscosity during pyrolysis identical at various T_{max} values.

The changes of the onset, end, and duration of swelling with T_{max} at a heating rate of 1×10^4 K/s and ambient pressure of 0.1 MPa are shown in Figure 12. At T_{max} lower than 910 K, when the particle reaches T_{max}, the amount of metaplast in the

DOI: 10.1021/acs.energyfuels.5b00609
Energy Fuels 2015, 29, 3953−3962

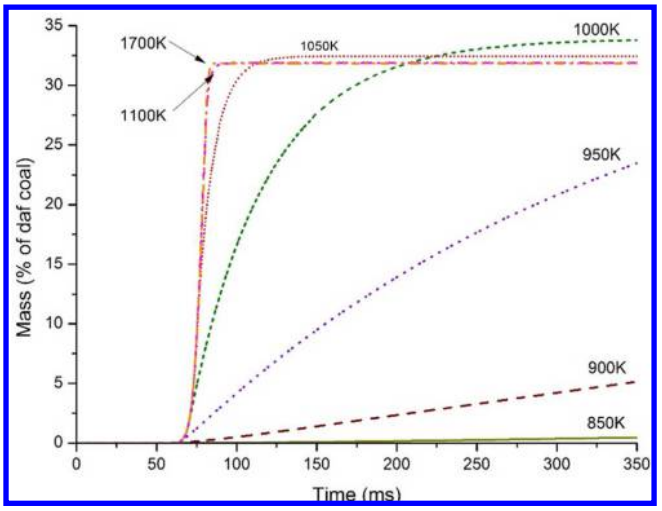

Figure 10. Predicted changes of metaplast cross-linked to the coal matrix during pyrolysis with increasing T_{max} (heating rate = 1×10^4 K/s, and ambient pressure = 0.1 MPa).

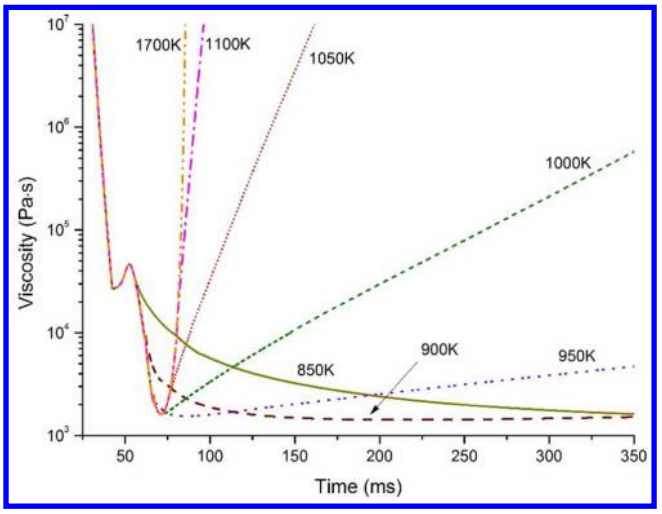

Figure 11. Predicted changes of the particle viscosity during pyrolysis with increasing T_{max} (heating rate = 1×10^4 K/s, and ambient pressure = 0.1 MPa).

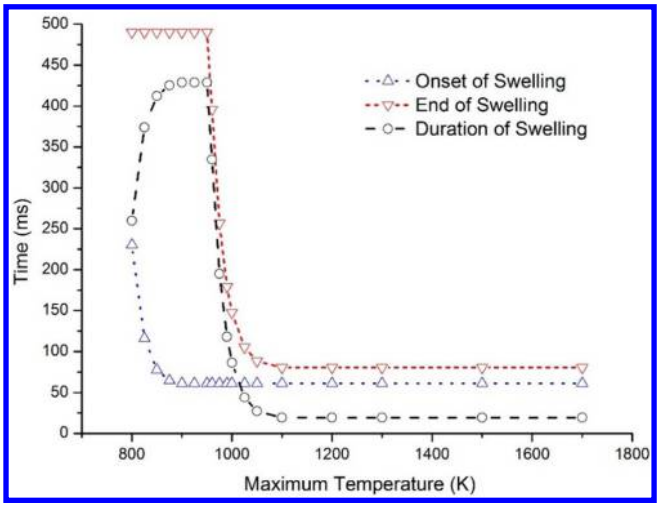

Figure 12. Change of the onset, end, and duration of swelling with T_{max} (heating rate = 1×10^4 K/s, and ambient pressure = 0.1 MPa).

particle is not high enough for swelling to occur. The particle will continue to react in a solid state at this temperature until the metaplast reaches a high enough concentration. Because the reaction rate increases with increasing temperature, at a higher T_{max}, more metaplast can be formed earlier, making the temperature at the onset of the swelling decrease with increasing T_{max}. However, at T_{max} larger than 910 K, the particle has become plastic before the particle reaches T_{max}, and therefore, the onset of the swelling does not change with further increases in T_{max}.

The vaporization rate is decreased with decreases in the temperature. At lower T_{max}, metaplast cannot vaporize in significant quantities and remains in the particle during pyrolysis, which delays the resolidification. Therefore, at T_{max} lower than 950 K, the end time of the swelling does not change with the increase of T_{max}. As T_{max} increases from 950 to 1100 K, the increasing vaporization rate of metaplast makes the swelling end earlier. At various T_{max} higher than 1100 K, because the changes of the particle viscosity with time during swelling are the same (see Figure 11), the end time of the swelling does not change with the further increase of T_{max}.

The changes of the onset and end of swelling with T_{max} make the duration of swelling first increase, then decrease, and finally remain constant with increasing T_{max}.

3.3.3. Influence of T_{max} on the Initial Bubble Number. At T_{max} lower than 910 K, the particle begins to swell at T_{max}. Increased T_{max} increases the reaction rate at the beginning of swelling, which, in turn, increases the initial bubble number. At T_{max} higher than 910 K, before the particle reaches T_{max}, the particle has been plastic. The temperatures at which the particle begins to swell do not change with T_{max}; therefore, the initial bubble number remains constant. The changes of the temperature at the onset of swelling and the initial bubble number in the particle with increasing T_{max} are shown in Figure 13.

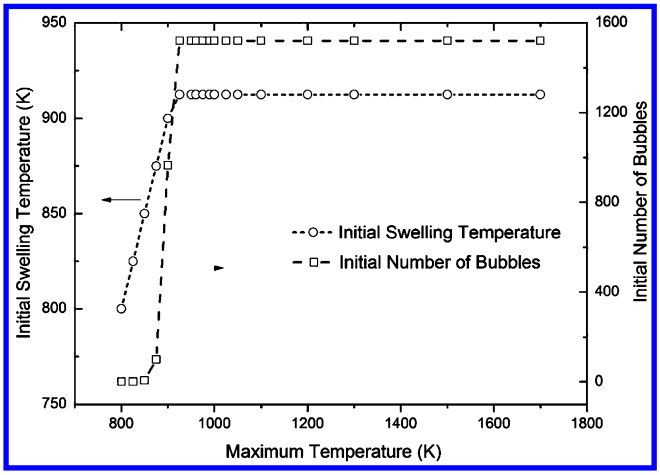

Figure 13. Changes of the swelling onset temperature and the initial bubble number in the plastic stage with increasing T_{max} (heating rate = 1×10^4 K/s, and ambient pressure = 0.1 MPa).

3.3.4. Sensitivity Analysis. The central bubble rupture frequency, the viscosity (μ_{coal}), and the initial bubble number (n_{b0}) all influence the swelling during pyrolysis. To find the dominant factor for the trend of swelling with increasing T_{max}, a brief sensitivity analysis was performed, as outlined in Table 4. In these computations, the heating rate was set to 1×10^4 K/s,

DOI: 10.1021/acs.energyfuels.5b00609
Energy Fuels 2015, 29, 3953−3962

Table 4. Conditions for Sensitivity Analysis

condition	S_w	μ_{coal}	t_{met0} and t_{mete}	n_{b0}
1	infinite (no rupture)	~[a]	~	~
2	~	$\mu_{coal} = \mu_{coal}^{1000\ K}$[b]	~	~
3	~	~	$t_{met0} = t_{met0}^{1000\ K}$, and $t_{mete} = t_{met0}^{1000\ K}$[c]	~
4	~	~	~	$n_{b0} = n_{b0}^{1000\ K}$[d]
5	~	~	~	~

[a]All values marked " ~ " chenge with T_{max}. [b]The change of coal viscosity during pyrolysis was set the same as at T_{max} = 1000 K. [c]The onset and end time of swelling were set the same as at T_{max} = 1000 K. [d]The initial bubble number during pyrolysis was set the same as at T_{max} = 1000 K.

and in each computation, one of the parameters was held constant at the value corresponding to T_{max} of 1000 K. Results of this sensitivity analysis are shown in Figure 14.

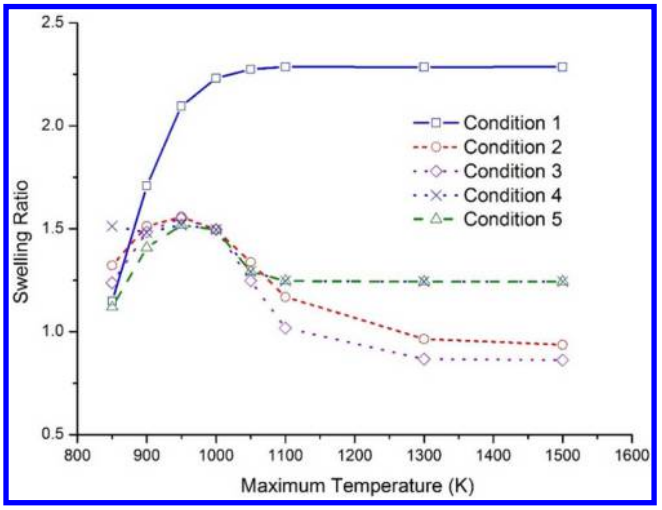

Figure 14. Results of sensitivity analysis (heating rate = 1×10^4 K/s, and ambient pressure = 0.1 MPa).

Under the condition that the central bubble did not rupture (condition 1), the final swelling ratio during pyrolysis increased from 1.15 to 2.29 with T_{max} increasing from 800 to 1100 K and then held constant, while under other conditions, the swelling ratios decreased with T_{max} increasing from 950 to 1100 K. This indicates that the increasing rupture frequency is the dominant factor for the decreasing trend of the swelling ratio with T_{max} increasing from 950 to 1100 K.

Under the condition that the initial bubble number was held constant (condition 4), the swelling ratio in general decreases from 1.51 to 1.24 as T_{max} increased from 800 to 1500 K, while under other conditions, the swelling ratios increased with T_{max} up to 950 K. This indicates that, at T_{max} lower than 950 K, the increasing initial bubble number with T_{max} is the dominant factor for the increasing trend of the swelling ratio.

Under the condition that the change of coal viscosity during pyrolysis was set the same as at T_{max} = 1000 K (condition 2) and under the condition that the onset and end times of swelling were set the same as at T_{max} = 1000 K (condition 3), the changes of swelling are different from the condition that all of the parameters change with T_{max} (condition 5). This indicates that the viscosity also influences the swelling.

An earlier end of swelling can decrease the rupture times and increase the swelling. Under condition 3, at various T_{max}, the end time of swelling was set to be the same as at T_{max} = 1000 K. Therefore, under condition 3, the end of swelling is earlier at T_{max} between 850 and 950 K than under condition 5 (see Figure 12), which increases the swelling. The end of swelling is later at T_{max} above 1100 K (see Figure 12), making the swelling smaller.

Under condition 2, the end time of swelling was the same as condition 3 but the change of particle viscosity was not the same. Under condition 2, the changes of coal viscosity during pyrolysis at various T_{max} values were set to be the same as at T_{max} = 1000 K. In Figure 11, the particle viscosity at T_{max} = 1000 K and 75 ms is smaller than at a T_{max} of 850−950 K. The particle viscosity at T_{max} = 1000 K is similar to that at T_{max} > 1100 K before 75 ms, but after 75 ms, the particle viscosity at T_{max} = 1000 K is smaller. At 75 ms, the volatile generation rate is highest during pyrolysis (see Figure 7), and therefore, the decreasing viscosity can increase the swelling, which, in turn, makes the swelling under condition 2 slightly larger than that under condition 3, as shown in Figure 14.

Under the condition that the viscosity evolution during pyrolysis changes with T_{max} (conditions 1 and 5), at T_{max} > 1100 K, because the changes of the particle viscosity with time during swelling (see Figure 11) and the initial bubble number in the plastic stage (see Figure 13) are the same, the swelling changes little with increasing T_{max}.

3.4. Influence of T_{max} at Various Heating Rates. At various heating rates, the particle swelling during pyrolysis increases with T_{max} up to about 950 K, decreases with T_{max} increasing from 950 to 1100 K, and then is kept constant with further increases in T_{max}, as shown in Figure 15.

At T_{max} < 1100 K, the changes of the heating rate and T_{max} influence the swelling together. At T_{max} higher than 1100 K, the influence of T_{max} on swelling is limited.

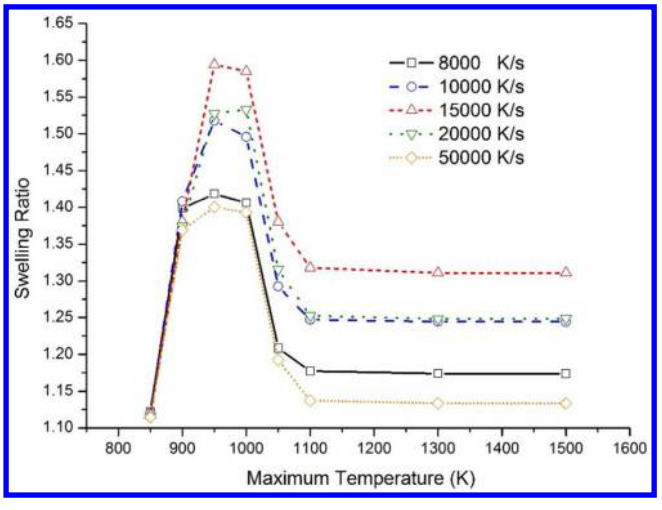

Figure 15. Change of the swelling ratio with increasing T_{max} at various heating rates (ambient pressure = 0.1 MPa).

DOI: 10.1021/acs.energyfuels.5b00609
Energy Fuels 2015, 29, 3953−3962

3.5. Influence of T_{max} at Various Ambient Pressures. At ambient pressures lower than 0.5 MPa, the swelling also first increases with increasing T_{max}, then decreases, and finally is kept constant at T_{max} > 1100 K. However, at ambient pressures higher than 0.5 MPa, because the rupture of the central bubble was restrained by the extra pressure, the swelling increases with increasing T_{max} up to about 1100 K and then remains constant, as shown in Figure 16.

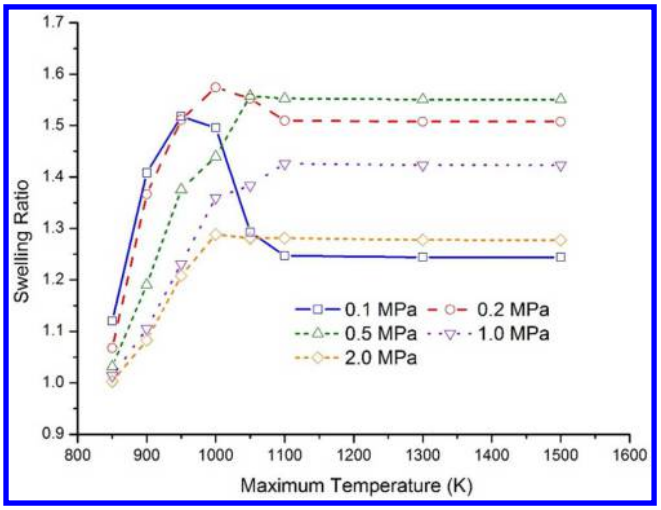

Figure 16. Change of the swelling ratio with increasing T_{max} at different ambient pressures (heating rate = 1×10^4 K/s).

At T_{max} > 950 K, the swelling ratio increases first and then decreases with increasing ambient pressure. A higher ambient pressure can restrain the central bubble rupture and increase the swelling, but too high of ambient pressure will counteract the pressure in the bubble and decrease both the tar release and the swelling.[17]

At T_{max} < 950 K, the swelling ratio decreases with increasing ambient pressure. At this temperature region, the volatile yield is small, which, in turn, decreases internal pressure and the bubble rupture frequency. With a smaller bubble rupture frequency, the restraining effect of the ambient pressure on bubble rupture is less obvious. However, the counteracting effect of the ambient pressure on a smaller internal pressure is more obvious.

4. CONCLUSION

An improved model for the swelling of high-volatile bituminous coal during pyrolysis was developed and evaluated. The swelling behavior of eight bituminous coals from the literature spanning a wide range of gas temperatures and gas pressures was predicted to test the suitability of the model.

At a constant heating rate of 1×10^4 K/s, the increase of the internal pressure and initial bubble number during the plastic stage causes the predicted particle swelling during pyrolysis to increase with T_{max} up to about 950 K. However, the increasing bubble rupture frequency makes the predicted swelling decrease as T_{max} increases from 950 to 1100 K. At T_{max} > 1100 K, before the particle reaches T_{max}, the particle resolidifies, and the temperature history during the plastic stage at various T_{max} values is the same, making the predicted swelling change little with further increases in T_{max}. At T_{max} < 1100 K, changes in T_{max} influence the predicted particle swelling ratio during pyrolysis. At T_{max} > higher than 950 K, the predicted swelling ratio increases first and then decreases with increasing ambient pressure. However, at T_{max} < 950 K, the predicted swelling ratio decreases with increasing ambient pressure.

AUTHOR INFORMATION

Corresponding Author

*E-mail: lisuf@dlut.edu.cn.

Notes

The authors declare no competing financial interest.

ACKNOWLEDGMENTS

This work is supported in part by a scholarship from the China Scholarship Council (CSC) under Grant CSC 201306060059 and performed at Brigham Young University while He Yang was a visiting graduate student.

NOMENCLATURE

A_{dry} = ash content on a dry basis
f_{CP} = initial volume fraction of closed pores in the parent particle
f_{gas} and f_{tar} = yield of gas and tar on a dry and ash-free basis, respectively
f_{VP} = influence factor of the particle volume on the initial bubble number
n_b = number of bubbles
P = pressure
P_∞ = ambient pressure
P_b = pressure in the bubble
p = fraction of intact bridges
R_p = radius of the particle
r_b = radius of the bubble
r_c = radius of the center bubble
S_w = critical wall stress
T_{max} = maximum particle temperature during pyrolysis
$\hat{V}_{pore}$ = volume of macropores
ϕ_m = metaplast content in the coal melt
μ_{coal} = viscosity of the coal particle
σ = surface tension
θ = porosity
ρ_{melted} = density of the melted coal

Superscripts andSubscripts

0 = initial condition of the plastic stage
b = bubble
p = particle
e = final condition of the plastic stage
m = average value
pc = parent coal

REFERENCES

(1) Bayless, D. J.; Schroeder, A. R.; Peters, J. E.; Buckius, R. O. Effects of surface voids on burning rate measurements of pulverized coal at diffusion-limited conditions. *Combust. Flame* **1997**, *108*, 187–198.

(2) Zeng, D.; Clark, M.; Gunderson, T.; Hecker, W. C.; Fletcher, T. H. Swelling properties and intrinsic reactivities of coal chars produced at elevated pressures and high heating rates. *Proc. Combust. Inst.* **2005**, *30*, 2213–2221.

(3) Bailey, J. G.; Tate, A.; Diessel, C. F. K.; Wall, T. F. A char morphology system with applications to coal combustion. *Fuel* **1990**, *69*, 225–239.

(4) Zygourakis, K. Effect of pyrolysis conditions on the macropore structure of coal derived chars. *Energy Fuels* **1993**, *7* (1), 33–41.

DOI: 10.1021/acs.energyfuels.5b00609
Energy Fuels 2015, 29, 3953–3962

(5) Gale, T. K.; Bartholomew, C. H.; Fletcher, T. H. Decreases in the swelling and porosity of bituminous coals during devolatilization at high heating rates. *Combust. Flame* **1995**, *100* (1−2), 94−100.
(6) Shurtz, R. C.; Kolste, K. K.; Fletcher, T. H. Coal swelling model for high heating rate pyrolysis applications. *Energy Fuels* **2011**, *25*, 2163−2173.
(7) Lee, C. W.; Scaroni, A. W.; Jenkins, R. G. Effect of pressure on the devolatilization and swelling behavior of a softening coal during rapid heating. *Fuel* **1991**, *70* (8), 957−965.
(8) Shurtz, R. C.; Hogge, J. W.; Fletcher, T. H. Coal swelling model for pressurized high particle heating rate pyrolysis applications. *Energy Fuels* **2012**, *26*, 3162−3627.
(9) Shurtz, R. C. Effects of pressure on the properties of coal char under gasification conditions at high initial heating rates. Ph.D. Dissertation, Brigham Young University, Provo, UT, 2011.
(10) Fletcher, T. H. Time-resolved temperature measurements of individual coal particles during devolatilization. *Combust. Sci. Technol.* **1989**, *63* (1−3), 89−105.
(11) Solomon, P. R.; Serio, M. A.; Hamblen, D. G.; Smoot, L. D.; Brewster, B. S.; Radulovic, P. T. *Measurement and Modeling of Advanced Coal Conversion Processes*; Advanced Fuel Reasearch, Inc. and Brigham Young University: East Hartford, CT, and Provo, UT, 1993; Final Report DE96000577, pp 71−73.
(12) Sheng, S.; Azevedo, J. L. T. Modeling the evolution of particle morphology during coal devolatilization. *Proc. Combust. Inst.* **2000**, *28*, 2225−2232.
(13) Oh, M. S.; Peters, W. A.; Howard, J. B. An experimental and modeling study of softening coal pyrolysis. *AIChE J.* **1989**, *35* (5), 775−792.
(14) Yu, J.; Strezov, V.; Lucas, J.; Liu, G.; Wall, T. A mechanistic study on char structure evolution during coal devolatilization—Experiments and model predictions. *Proc. Combust. Inst.* **2002**, *29* (1), 467−473.
(15) Yu, J.; Lucas, J.; Wall, T. Modeling the development of char structure during the rapid heating of pulverized coal. *Combust. Flame* **2004**, *136*, 519−532.
(16) Griffin, T. P.; Howard, J. B.; Peters, W. A. An experimental and modeling study of heating rate and particle size effects in bituminous coal pyrolysis. *Energy Fuels* **1993**, *7* (2), 297−305.
(17) Yang, H.; Li, S.; Fletcher, T. H.; Dong, M. Simulation of the swelling of high-volatile bituminous coal during pyrolysis. *Energy Fuels* **2014**, *28* (11), 7216−7226.
(18) Yang, H.; Li, S.; Fletcher, T. H.; Dong, M.; Zhou, W. Simulation of the evolution of pressure in a lignite particle during pyrolysis. *Energy Fuels* **2014**, *28* (5), 3511−3518.
(19) Fletcher, T. H.; Hardesty, D. R. *Compilation of Sandia Coal Devolatilization Data: Milestone Report*; Sandia National Laboratories: Livermore, CA, 1992; SAND92-8209, pp 5−43.
(20) Gale, T. K. Effects of pyrolysis condition on coal char properties. Ph.D. Dissertation, Brigham Young University, Provo, UT, 1994.
(21) Grant, D. M.; Pugmire, R. J.; Fletcher, T. H.; Kerstein, A. R. Chemical model of coal devolatilization using percolation lattice statistics. *Energy Fuels* **1989**, *3*, 175−186.
(22) Fletcher, T. H.; Kerstein, A. R.; Pugmire, R. J.; Grant, D. M. Chemical percolation model for devolatilization. 2. Temperature and heating rate effects on product yields. *Energy Fuels* **1990**, *4*, 54−60.
(23) Fletcher, T. H.; Kerstein, A. R.; Pugmire, R. J.; Solum, M. S.; Grant, D. M. Chemical percolation model for devolatilization. 3. Direct use of ^{13}C NMR data to predict effects of coal type. *Energy Fuels* **1992**, *6* (4), 414−431.
(24) Fong, W. S.; Peters, W. A.; Howard, J. B. Kinetics of generation and destruction of pyridine extractables in a rapidly pyrolysing bituminous coal. *Fuel* **1986**, *65* (2), 251−254.
(25) Fong, W. S.; Khalil, Y. F.; Peters, W. A.; Howard, J. B. Plastic behaviour of coal under rapid-heating high-temperature conditions. *Fuel* **1986**, *65* (2), 195−201.
(26) Gan, H.; Nandi, S. P.; Walker, P. L. Nature of the porosity in American coals. *Fuel* **1972**, *51*, 272−277.
(27) Genetti, D. B. An advanced model of coal devolatilization based on chemical structure. M.S. Thesis, Brigham Young University, Provo, UT, 1999.

DOI: 10.1021/acs.energyfuels.5b00609
Energy Fuels 2015, 29, 3953−3962